Cell Stem Cell
Article

Oct4 Expression Is Not Required for Mouse Somatic Stem Cell Self-Renewal

Christopher J. Lengner,[1] Fernando D. Camargo,[1] Konrad Hochedlinger,[3] G. Grant Welstead,[1] Samir Zaidi,[2] Sumita Gokhale,[1] Hans R. Scholer,[4] Alexey Tomilin,[5] and Rudolf Jaenisch[1,2,*]
[1]Whitehead Institute for Biomedical Research
[2]Department of Biology
Massachusetts Institute of Technology, 9 Cambridge Center, Cambridge, MA 02142, USA
[3]Massachusetts General Hospital Cancer Center and Center for Regenerative Medicine, Harvard Stem Cell Institute, 185 Cambridge Street, Boston, MA 02114, USA
[4]Department of Cell and Developmental Biology, Max Planck Institute for Molecular Biomedicine, Röntgenstrasse 20, 48149 Münster, Germany
[5]Institute of Cytology, Russian Academy of Science, 4 Tikhoretski Avenue, 194064 St-Petersburg, Russia
*Correspondence: jaenisch@wi.mit.edu
DOI 10.1016/j.stem.2007.07.020

SUMMARY

The Pou domain containing transcription factor *Oct4* is a well-established regulator of pluripotency in the inner cell mass of the mammalian blastocyst as well as in embryonic stem cells. While it has been shown that the *Oct4* gene is inactivated through a series of epigenetic modifications following implantation, recent studies have detected *Oct4* activity in a variety of somatic stem cells and tumor cells. Based on these observations it has been suggested that *Oct4* may also function in maintaining self-renewal of somatic stem cells and, in addition, may promote tumor formation. We employed a genetic approach to determine whether *Oct4* is important for maintaining pluripotency in the stem cell compartments of several somatic tissues, including the intestinal epithelium, bone marrow (hematopoietic and mesenchymal lineages), hair follicle, brain, and liver. *Oct4* gene ablation in these tissues revealed no abnormalities in homeostasis or regenerative capacity. We conclude that *Oct4* is dispensable for both self-renewal and maintenance of somatic stem cells in the adult mammal.

INTRODUCTION

The transcriptional regulator *Oct4* is a Pou domain containing protein expressed in pluripotent embryonic cells and cells of the germline where its inactivation results in loss of pluripotency and apoptosis, respectively (Kehler et al., 2004; Nichols et al., 1998). In embryonic stem (ES) cells, *Oct4*, along with transcriptional coregulators *Nanog* and *Sox-2*, orchestrates a program of gene activity that suppresses differentiation while endowing self-renewal (Boyer et al., 2005; Loh et al., 2006; Wang et al., 2006). Upon induction of differentiation, the *Oct4* locus undergoes a series of repressive epigenetic modifications mediated by the histone methyltransferase *G9a* and the de novo DNA methyltransferases *DNMT3a/b* (Feldman et al., 2006). Recent studies have, however, shown that *Oct4* is active in a variety of somatic stem cell compartments and in cultured multipotent somatic progenitor cells, where it has been suggested to function in a manner analogous to its role in ES cells (see Table S1 in the Supplemental Data available with this article online). Consistent with this possibility is the observation that ectopic expression of *Oct4* in mice harboring a single-copy, doxycycline-inducible transgene is sufficient to prevent differentiation of intestinal epithelium while concomitantly stimulating expansion of the progenitor cell compartment (Hochedlinger et al., 2005).

Oct4 gene expression in the adult has been most frequently reported in the bone marrow of both humans and mice, particularly in hematopoietic and mesenchymal stem cells (HSCs and MSCs) (D'Ippolito et al., 2004, 2006; Goolsby et al., 2003; Izadpanah et al., 2006; Jiang et al., 2002; Johnson et al., 2005; Lamoury et al., 2006; Moriscot et al., 2005; Nayernia et al., 2006; Pallante et al., 2007; Pochampally et al., 2004; Ren et al., 2006), as well as in various subpopulations of multipotent progenitors (D'Ippolito et al., 2004, 2006; Jiang et al., 2002; Nayernia et al., 2006; Pallante et al., 2007; Serafini et al., 2007; Zhang et al., 2005). Additionally, *Oct4* expression has been detected in progenitor cells from other tissues, including pancreatic islets (Wang et al., 2004), kidney (Gupta et al., 2006; Sagrinati et al., 2006), peripheral blood (Johnson et al., 2005; Romagnani et al., 2005; Tondreau et al., 2005), mammary epithelium (Tai et al., 2005), endometrium of the uterus (Cervello et al., 2006; Matthai et al., 2006), thyroid (Thomas et al., 2006), lung (Ling et al., 2006), brain (Davis et al., 2006; Okuda et al., 2004), liver (Beltrami et al., 2007), dermis, and hair follicles (Dyce et al., 2004, 2006; Kues et al., 2005; Mongan et al., 2006; Redvers et al., 2006; Yu et al., 2006). In addition to these tissues,

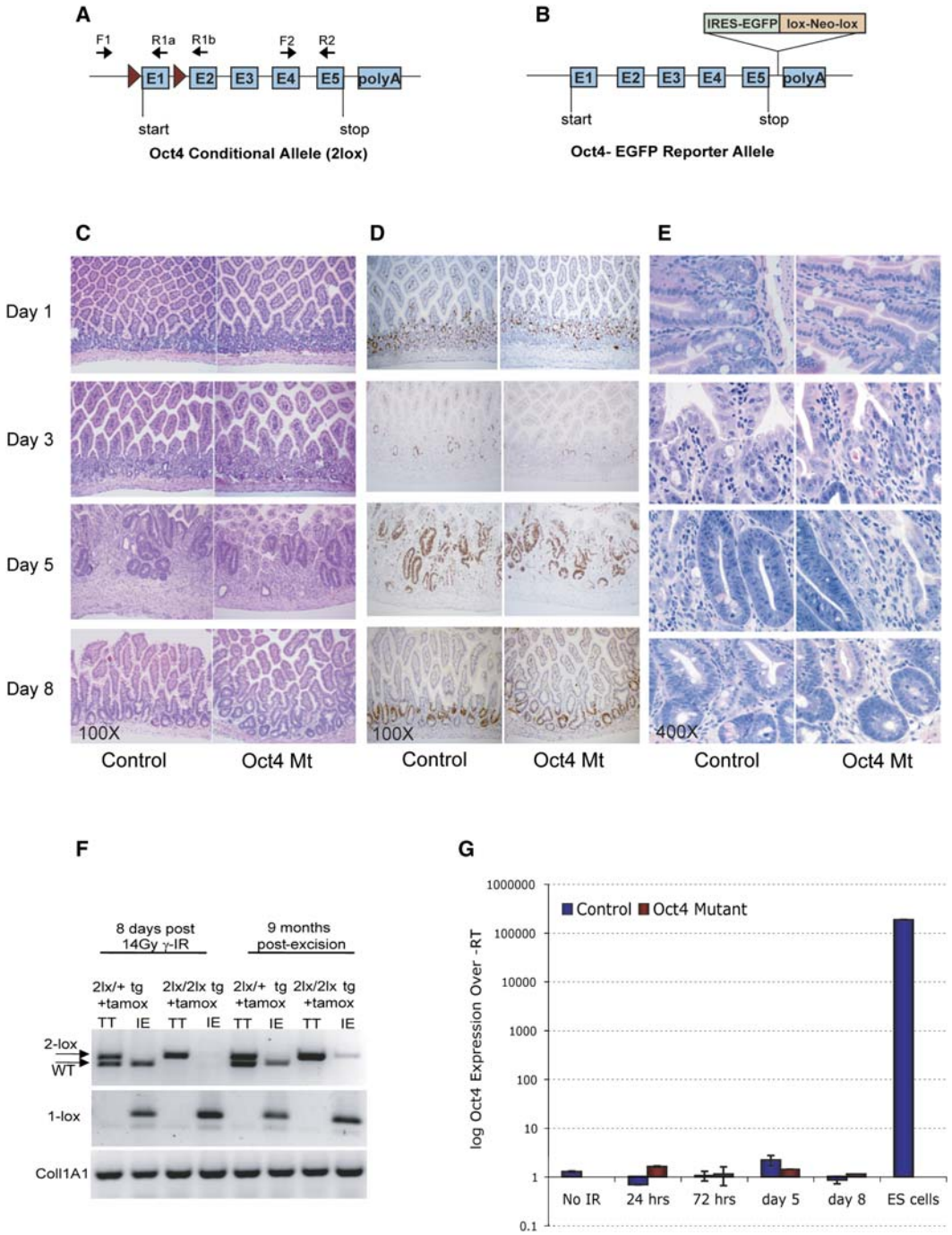

Figure 1. Regeneration of the Intestinal Epithelium after *Villin-CreER*-Mediated *Oct4* Inactivation

(A) Schematic of the *Oct4* conditional allele subjected to Cre-mediated recombination. Primer sets F1/R1a and F1/R1b were used for verification of excision, detecting the 2-lox and 1-lox alleles, respectively. Primer set F2/R2 spanning exons 4 and 5 was used for qRT-PCR analysis.

(B) Schematic of the *Oct4-EGFP* reporter allele used to assess *Oct4* gene activity.

(C) Hematoxylin- and eosin-stained paraffin sections of intestinal epithelium radio-ablated with 14 Gy γ irradiation show cell death 3 days post-irradiation, followed by regeneration within 5 days and a morphologically normal crypt-villus structure 8 days after γ irradiation.

(D) Ki67 staining of sections in (C) shows that the proliferative zone at the base of the villi undergoes cell-cycle arrest by 3 days post-γ irradiation, followed by increased proliferation at 5 days. Eight days after γ irradiation, the proliferative zone returns to the normal state.

(E) Higher magnification of (A) showing cells with abnormal nuclear morphology consistent with apoptosis 3 days after γ irradiation. Newly generated crypt cells exhibit normal morphology with basal nuclei.

(F) PCR analysis of genomic DNA isolated from tail tip (TT) or intestinal epithelium (IE) after Villin-Cre activation and either 8 days after γ irradiation (γ-IR) or 9 months after excision. Loss of the 2-lox (functional) allele and appearance of the 1-lox (inactive) allele indicate successful recombination. The type I collagen locus is a loading control.

Table 1. Cre-Expressing Mouse Lines Used for Tissue-Specific *Oct4* Deletion

Cre Transgene/Affected Tissue	Temporal Induction of Oct4 Excision	Excision Efficiency
Villin-CreER/intestinal epithelium	Tamoxifen inducible	~100% (el Marjou et al., 2004)
Keratin15-CrePr1/hair follicle bulge stem cells	Mifepristone (RU486) inducible	~100% (Morris et al., 2004)
Mx1Cre/hematopoetic lineages	Interferon (poly dI/dC) inducible	~100% (Kuhn et al., 1995)
Mx1Cre/marrow stromal cells	Interferon (poly dI/dC) inducible	>95%
Mx1Cre/hepatocytes	Interferon (poly dI/dC) inducible	>90%
Nestin-Cre neural progenitor cells	E9.5–E15.5	~100% (Bates et al., 1999)

a number of studies have reported *Oct4* expression in primary tumors, transformed cells, amniotic fluid, and umbilical cord blood (see Table S1 for references). Given its expression in a variety of normal tissues and transformed cells, it has been suggested that *Oct4* may not only be crucial for the maintenance of pluripotency in embryonic cells but may also play an important role for the self-renewal of somatic stem cells and in maintaining tissue homeostasis. The goal of the current study was to test this hypothesis by deleting *Oct4* from somatic stem cell compartments in vivo.

RESULTS

To investigate a possible function of *Oct4* expression in somatic cells, we used a Cre-lox based recombination approach to achieve tissue-specific inactivation of a conditional *Oct4* allele (*Oct4-2lox*, Figure 1A) (Kehler et al., 2004). *Oct4-2lox* mice were crossed to mice carrying tissue-specific or inducible Cre transgenes to inactivate *Oct4* in organs that have a well-defined somatic stem cell population. We deleted *Oct4* in the intestine, bone marrow, brain, liver, and hair follicles because *Oct4* expression has previously been documented in these tissues (Table S1). The Cre transgenes that were used to achieve cell-type-specific deletion of *Oct4* in these tissues are described in Table 1.

Intestinal Epithelium

Inactivation of *Oct4* in the intestinal epithelium (including progenitor cells residing in the intestinal crypt) was achieved through the tamoxifen-induced activation of a transgene encoding a Cre recombinase/estrogen receptor fusion protein under transcriptional control of the *Villin* promoter (*Villin-CreER*) (el Marjou et al., 2004) in 8-week-old mice. Recombination of the *Oct4-2lox* allele was confirmed by Southern blot analysis (data not shown). Weight gain was monitored in adult mice for a period of 9 months, with no differences observed between control ($Oct4^{1lox/+}$, *transgenic*) and *Oct4* mutant ($Oct4^{1lox/1lox}$, *transgenic*) mice (Figure S1). Histological analysis revealed a normal tissue architecture containing differentiated cell types (Paneth and goblet cells), a normal distribution of proliferating cells marked by Ki67 expression, and an absence of any Oct4-positive cells in the crypts (Figure S1). In order to test the regenerative capacity of intestinal crypt progenitor cells in the absence of *Oct4*, mice were subjected to a 14 Gy dose of γ irradiation. This resulted in widespread apoptosis and cell death coupled with a growth arrest within 3 days. Five days after γ irradiation, intestinal progenitor cells became highly proliferative in the presence or absence of *Oct4*, giving rise to new crypts that reestablished a normal intestinal epithelium by the eighth day after irradiation (Figures 1C–1E). In order to exclude the possibility that a small number of progenitor cells escaped recombination and were responsible for the observed regeneration and maintenance of the intestinal epithelium, we performed PCR analysis of the *Oct4* genomic locus. This analysis revealed no evidence of nonrecombined *Oct4-2lox* alleles in the newly generated tissue (Figure 1F). Finally, we examined *Oct4* gene expression throughout the time course of epithelial recovery after irradiation and found little to no *Oct4* mRNA. *Oct4* expression in the intestine was found to be 10^5 times lower in comparison to ES cells (Figure 1G). Further purification of crypt progenitor cells by EDTA-based fractionation of intestinal epithelium followed by gene expression analysis revealed no preference for Oct4 expression at the base of the crypt (Figure S1). These findings indicate that *Oct4* function is not required for maintenance of the intestinal stem cell niche.

Mesenchymal Stem Cells

In order to examine the effects of *Oct4* deletion in the bone marrow, we employed an interferon-inducible *Mx1-Cre* transgene (Table 1) (Kuhn et al., 1995; Schneider et al., 2003). We confirmed that activation of *Mx1-Cre* resulted in 100% recombination in the whole marrow by PCR analysis (Figure 2A). Subsequent separation of mesenchymal and hematopoietic cells confirmed recombination in both cell lineages (data not shown). MSCs known to give rise to cells of chondrogenic, adipogenic, myogenic, and

(G) Quantitative RT-PCR throughout the time course of intestinal regeneration. Data are displayed as average signal intensity ± SD relative to a control lacking reverse transcriptase (−RT).

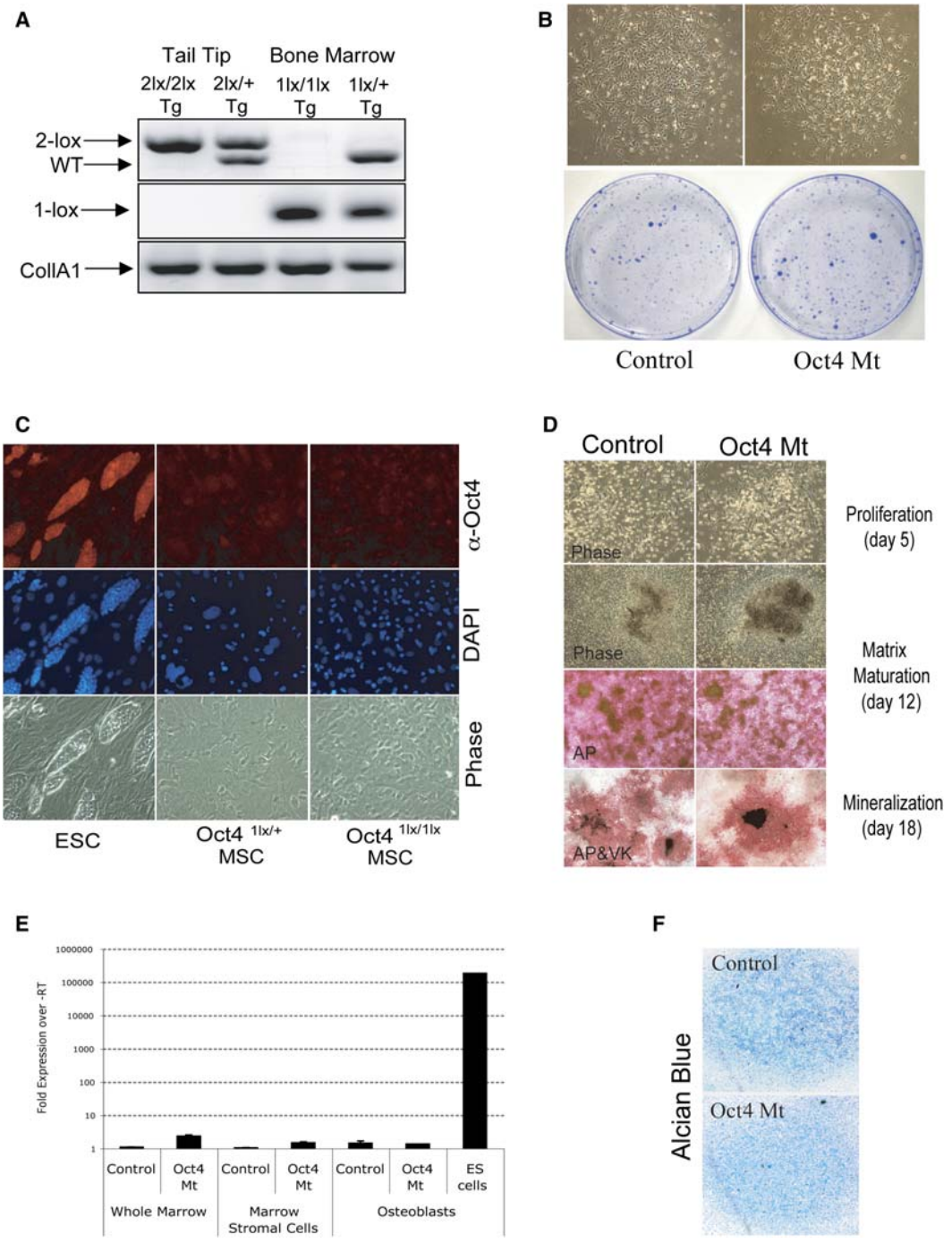

Figure 2. Proliferative and Lineage Commitment Capacity of Bone Marrow-Derived MSCs after *Mx1-Cre*-Mediated Inactivation of *Oct4*

(A) Complete excision of the conditional *Oct4* allele was validated in whole bone marrow as described in Figure 1.

(B) MSC clonal colony formation assay 5 days after marrow isolation.

(C) MSC colonies do not exhibit any significant *Oct4* immunoreactivity in comparison to ES cell colonies.

(D) MSCs isolated from control and *Oct4* mutant bone marrow cultured under osteogenic conditions formed postconfluent multilayered nodules that express the early osteogenic marker *Alkaline Phosphatase* (AP) (day 12). By 18 days of culture mature osteoblasts form mineralized extracellular matrix detected by silver nitrate staining per the method of Von Kossa (VK).

(E) Quantitative RT-PCR analysis of *Oct4* expression in primary whole marrow, proliferating MSCs, and differentiated osteoblasts as described in Figure 1G.

(F) Chondrogenic, high-density micromass cultures of MSCs form negatively charged extracellular matrix stained by Alcian blue.

osteogenic lineages (Keating, 2006) were derived from both control and mutant bone marrow. These cells, as well as multipotent subpopulations of MSCs, have been the most frequently cited source of *Oct4* expression in somatic tissues (Table S1). The proliferative capacity and potential for lineage commitment of MSCs were addressed using in vitro colony formation assays, osteoblast and chondrocyte differentiation assays. Individual MSCs derived from both control and Oct4 mutant MSCs were able to proliferate to form clonal colonies (Figure 2B). Upon reaching confluence, these cells underwent osteogenic differentiation in the presence of ascorbic acid and inorganic phosphate, forming multilayered nodules containing mineralized extracellular matrix hallmarks of mature osteoblasts (Figure 2D). No *Oct4*-positive cells were observed during colony formation (Figure 2C). Gene expression analysis throughout the time course of osteogenic lineage commitment revealed no significant *Oct4* gene activity in whole marrow, proliferating MSCs, or in differentiated osteoblasts (Figure 2E). Similarly, *Oct4* mutant MSCs were able to activate *Sox9* gene expression and enter the chondrogenic lineage in BMP-treated micromass cultures (Figure 2F and Figure S2).

Hematopoietic Lineages

Oct4 function was addressed in the well-defined HSC (Kondo et al., 2003). Examination of the peripheral blood circulation of control and *Oct4* mutant mice 5, 12, and 35 days after *Mx1-Cre* induced recombination revealed no deficiency in the ability of *Oct4* mutant mice to maintain white blood cell (WBC), red blood cell (RBC), or platelet counts at control levels throughout the experiment (Figures 3A and 3B). Flow cytometric analysis of the bone marrow for monocyte, B cell, and granulocyte lineages at 12 and 35 days after recombination showed little difference in the representation of these cell types between control and *Oct4* mutant animals (Figure 3C and data not shown). Furthermore, *Oct4* deletion did not affect the lineage-negative, *c-kit*+, *sca1*+ population of HSCs in the bone marrow (Figure 3D) (Camargo et al., 2006). Subsequent analysis of *Flt3*-negative long-term HSCs and *Flt3*-positive short-term HSCs showed no variation in these populations in the absence of *Oct4* (data not shown). Quantitative RT-PCR (qRT-PCR) analysis of flow-sorted HSCs, common lymphoid progenitors, granulocytes, and monocytes revealed no preference for *Oct4* expression in stem cells, and expression in all of these cell types was negligible in comparison to ES cells (Figure S2). PCR analysis for the *2-lox* and recombined *1-lox Oct4* alleles 8 weeks after *Mx1-Cre* activation verified the persistence of *Oct4* null cells in the marrow, ruling out potential functional contribution of any cells escaping Cre-mediated recombination (Figure 3E). Ultimately, we tested the regenerative potential of the HSCs by performing a competitive reconstitution assay in which equal numbers of either control or *Oct4* mutant marrow cells bearing a CD45.1 cell surface antigen were isolated 5 days after *Mx1-Cre* activation and coinjected along with CD45.2 competitor cells into lethally irradiated recipient mice. The CD45.1 and CD45.2 cells were allowed to compete for reestablishment of the recipient's hematopoietic system, and the relative contribution of each donor cell was assessed (Figure 3F). We found no significant differences in the ability of control or *Oct4* mutant cells to repopulate the ablated hematopoietic systems of recipient animals. Moreover, the observed reconstitution was stable over time, demonstrating that HSCs lacking functional *Oct4* alleles fully retain long-term pluripotency.

Liver

While a clearly defined stem cell niche has not been identified in the liver, several candidate progenitor cells have been described (Walkup and Gerber, 2006) and *Oct4* has been observed in liver-derived stem cells (Beltrami et al., 2007). To test whether *Oct4* functions in liver regeneration, we performed partial hepatectomies after inactivation of *Oct4* using *Mx1-Cre* (Kuhn et al., 1995; Schneider et al., 2003) (Figure 4A). Two months after removal of 75% of the liver, both control and *Oct4* mutant mice were able to fully regenerate lost tissue. The newly generated liver was histologically normal, containing mature hepatocytes, bile ducts, and vascularization (Figure 4B). In addition, *Oct4* protein was undetectable by immunostaining and little to no *Oct4* mRNA was expressed in the regenerated liver (Figures 4C and 4D). As in the intestinal epithelium, the newly regenerated liver of *Oct4* mutant mice lacked nonrecombined *Oct4-2lox* alleles (Figure 4E), demonstrating that cells lacking functional *Oct4* alleles are capable of tissue regeneration.

Brain

The *Oct4* zebrafish ortholog *spiel ohne grenzen* (*spg*) has been shown to be necessary for formation of the mid- and hindbrain (Belting et al., 2001), and cultures of mammalian neural progenitors exhibit *Oct4* expression (Davis et al., 2006; Okuda et al., 2004). We therefore examined the effect of *Oct4* deletion in neural progenitor cells. A paternally transmitted *Nestin-Cre* transgene was used to excise the *Oct4* conditional allele in all neural progenitor cells of the developing brain (Table 1) (Bates et al., 1999; Fan et al., 2001). *Oct4* mutant mice exhibited no apparent behavioral abnormalities and brain morphology appeared normal more than one year after *Oct4* deletion (Figure 5A). Ki67-positive neural stem cells were seen in the subventricular zone of the lateral ventricles of both control and *Oct4* mutant mice (Figures 5A and 5B). Oct4 expression in this region was undetectable by immunostaining (Figures 5A and 5B), and *Oct4* mRNA was nearly undetectable in both control and mutant brain extract, embryonic day 13 brain extract, as well as in purified primary cultures of neural progenitor cells (Figure 5C).

Hair Follicle

The function of *Oct4* was examined in the hair follicle through activation of a *Keratin1-15 CrePr1* transgene (*K15-CrePr1*). This transgene encodes a Cre-progesterone receptor fusion protein and is expressed exclusively in the hair follicle bulge stem cells (Morris et al., 2004).

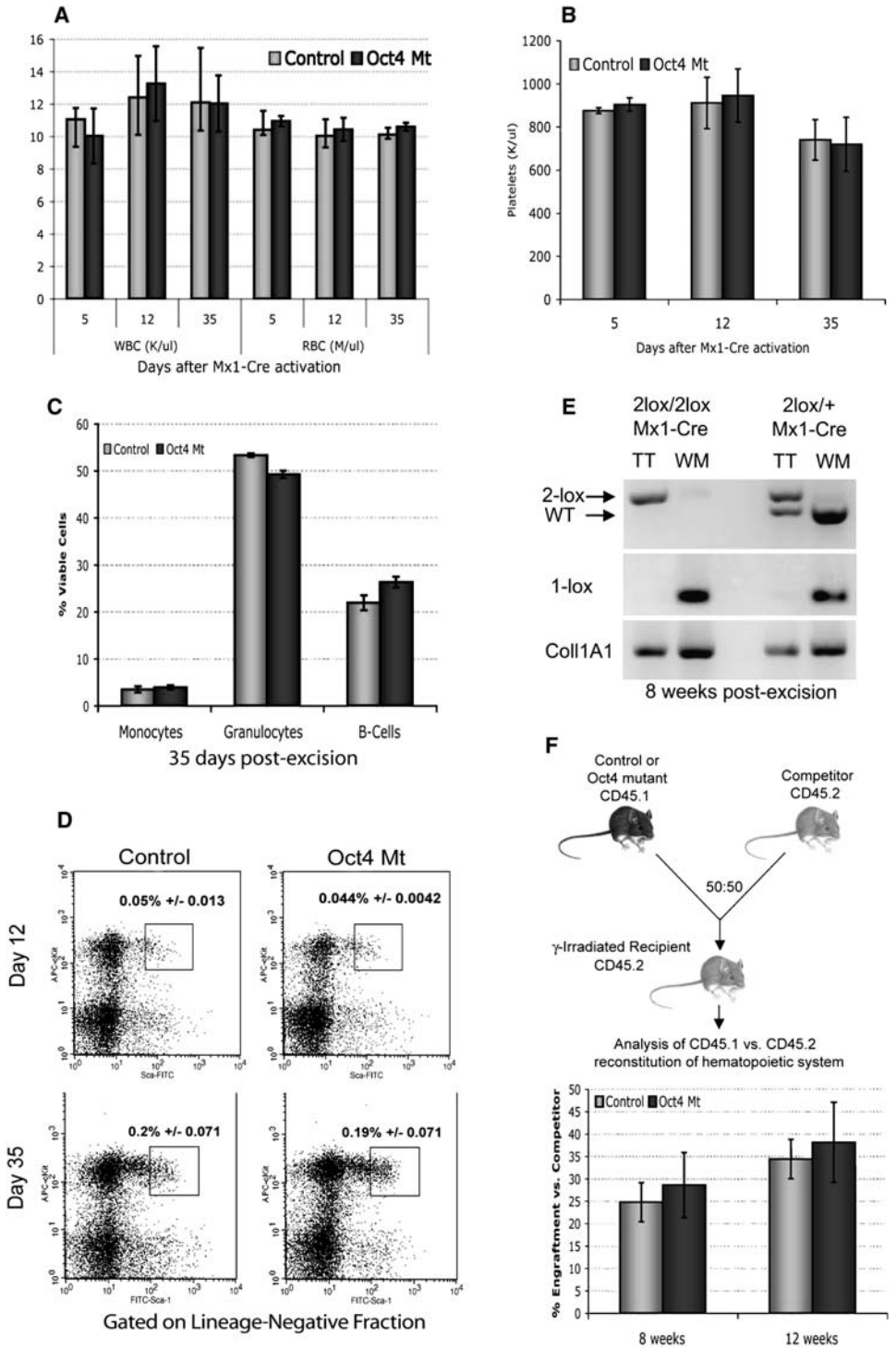

Figure 3. Hematopoietic Lineage Analysis in *Mx1-Cre*, *Oct4* Conditional Mice

(A) Analysis of peripheral blood from control or *Oct4* mutant mice 5, 12, and 35 days after inactivation of the *Oct4* gene with *Mx1-Cre*. White blood cell (WBC) and red blood cell (RBC) counts were unaffected in the absence of *Oct4*.

(B) Platelet counts 5, 12, and 35 days after *Oct4* inactivation. Data are presented as mean ± SD, n = 5.

(C) Staining of whole marrow 35 days after Cre-mediated excision with hematopoietic lineage markers for granulocytes, monocytes, and B cells isolated from bone marrow and analyzed by flow cytometry.

(D) HSC markers c-Kit and Sca1 allow for the visualization of c-Kit+, Sca1+ HSCs by flow cytometry gated on the lineage-negative (lin−) fraction of viable cells at 12 and 35 days after *Oct4* inactivation. Data presented as mean ± SD, n = 3.

(E) Analysis of genomic DNA isolated from bone marrow (WM) 8 weeks after excision of the conditional *Oct4* allele with *Mx1-Cre* demonstrating stability of *Oct4* null cells in the marrow. Tail tip genomic DNA (TT) shows nonrecombined controls.

These cells give rise to all differentiated cell types in the follicle, enter the dermal lineage during wound healing (Ito et al., 2005), and have previously been shown to express *Oct4* (Yu et al., 2006). The hair follicles of 8-week-old mice were examined after activation of *K15-CrePr1* through dermal administration of the progesterone antagonist mifepristone. We observed differentiated cell types and sebaceous glands in both control and *Oct4* mutant follicles (Figure 5D). Immunostaining with Oct4 and Ki67 antibodies revealed no Oct4-positive cells in or around the follicle and a normal distribution of proliferating cells (Figure 5D), and qRT-PCR analysis of mRNA isolated from skin revealed no significant *Oct4* expression relative to ES cells (Figure 4D). To test the regenerative capacity of the skin in control and *Oct4* mutant mice, we performed wound-healing assays in which 8 mm, full-thickness dermal biopsies were monitored for 2 weeks and found no significant differences in wound-healing capacity (Figure 5E). While recent studies have demonstrated that an additional epidermal stem cell, which may or may not have inactivated *Oct4* in our model, can contribute to wound healing and follicle formation after wounding, our *Oct4 K15-CrePr1* mice were able to continue hair growth during homeostatic conditions, a process known to be dependent on the *K15*-positive stem cells of the follicular bulge (Morris et al., 2004).

Oct4 Expression in Somatic Cells

The results described thus far failed to reveal any functional role for *Oct4* in the homeostasis or regeneration of a number of somatic tissues. Because *Oct4* expression in somatic tissues has been detected in stem cell populations by PCR or immunohistological methods in a number of published reports (Table S1), we attempted to confirm these observations using another approach. We generated a reporter allele through homologous recombination in ES cells in which *EGFP* is expressed from the endogenous *Oct4* locus (*Oct4-EGFP*) (Figure 1B). The fidelity of the reporter was confirmed by flow cytometric analysis of targeted ES cells. Over 95% of *Oct4-EGFP* ES cells strongly expressed *EGFP*, consistent with their pluripotent state (Figure 6A). We subsequently generated mice from *Oct4-EGFP* ES cells and examined *EGFP* expression at the single cell level in a number of tissues. Flow cytometric analysis of whole bone marrow containing multipotent MSCs and HSCs revealed no *EGFP*-positive cell population when compared to wild-type marrow (Figure 6B). Purification of c-kit+, sca1+, lineage− HSCs derived from the bone marrow confirmed the absence of *Oct4*-expressing hematopoietic progenitors (Figure 6C). In addition to the bone marrow, numerous other tissues, including liver, brain, intestine, stomach, skeletal muscle, skin, lungs, heart, spleen, kidney, bladder, thymus, and prostate were examined using antibodies raised against *EGFP* and positive signals were never observed, in contrast to teratomas derived from *Oct4-EGFP* ES cells, which exhibit pockets of undifferentiated cells with strong GFP expression (Figure S3 and data not shown). These findings, coupled with the failure to detect *Oct4* transcripts by qRT-PCR, indicate that the endogenous *Oct4* locus is inactive in the adult mouse. Our results are consistent with the *Oct4* locus being effectively silenced in somatic tissues and therefore dispensable for the maintenance of somatic stem cells or tissue regeneration in the adult.

DISCUSSION

Oct4 expression in somatic stem cells and in various cancer cells has been described in numerous recently published reports (Table S1). This has led to the provocative proposition that *Oct4* may be involved not only in the maintenance of pluripotency in ES cells but also in the self-renewal of somatic stem cells and in the genesis of cancers (Tai et al., 2005). To test this possibility, we deleted the *Oct4* gene in several tissues that have well-defined stem cell compartments and a high rate of cell turnover. *Oct4* deletion in the intestine, bone marrow, hair follicle, liver, or CNS had no effect on tissue maintenance or injury-induced regeneration. Moreover, we observed no significant expression of the *Oct4* gene using immunohistochemistry, quantitative RT-PCR, or flow cytometric analysis of cells harboring a targeted *Oct4-EGFP* reporter allele.

While *Oct4* is highly expressed in ES cells, it becomes silenced upon differentiation through a two-step mechanism in which histone H3 methylation precedes Dnmt3a/3b-mediated promoter methylation (Feldman et al., 2006). *Oct4* activity does, however, persist in the germline, where it is required for the viability of germ cells (Kehler et al., 2004). Furthermore, *Oct4* is frequently expressed in tumors of germ cell origin, where it acts as an oncogenic fate determinant (Gidekel et al., 2003; Looijenga et al., 2003). It is significant for this discussion that ectopic activation of *Oct4* in the intestine or skin results in rapid expansion of progenitor cells and invasive tumor formation indicating that *Oct4* can also act as a powerful oncogene in somatic cells (Hochedlinger et al., 2005). If *Oct4* functioned in somatic stem cells and the *Oct4* genomic locus existed in a state permissible for transcriptional activation in these cells, one might expect that it would be a frequently activated oncogene in cancers of somatic origin. This, however, does not seem to be the case. Looijenga et al. examined the expression of *Oct4* in over 3600 primary tumors representing more than 100 tumor types and found *Oct4* reactivity consistently in germ cell tumors, but only in three tumors of somatic origin (Looijenga et al., 2003). In these rare *Oct4*-expressing somatic tumors, *Oct4* expression could potentially be due to genomic rearrangements transposing the *Oct4* coding sequence into the vicinity of active promoter regions rather than

(F) Competitive reconstitution assay in which control or *Oct4* mutant marrow cells were isolated 5 days after *Mx1-Cre*-mediated excision of *Oct4* and each injected into lethally irradiated recipient mice along with an equal number of isogenic competitor cells. Donor and competitor cells were isolated from peripherial blood at 8 and 12 weeks after transplant and distinguished by CD45 isotypes. Data are presented as mean values ± SD, n = 10.

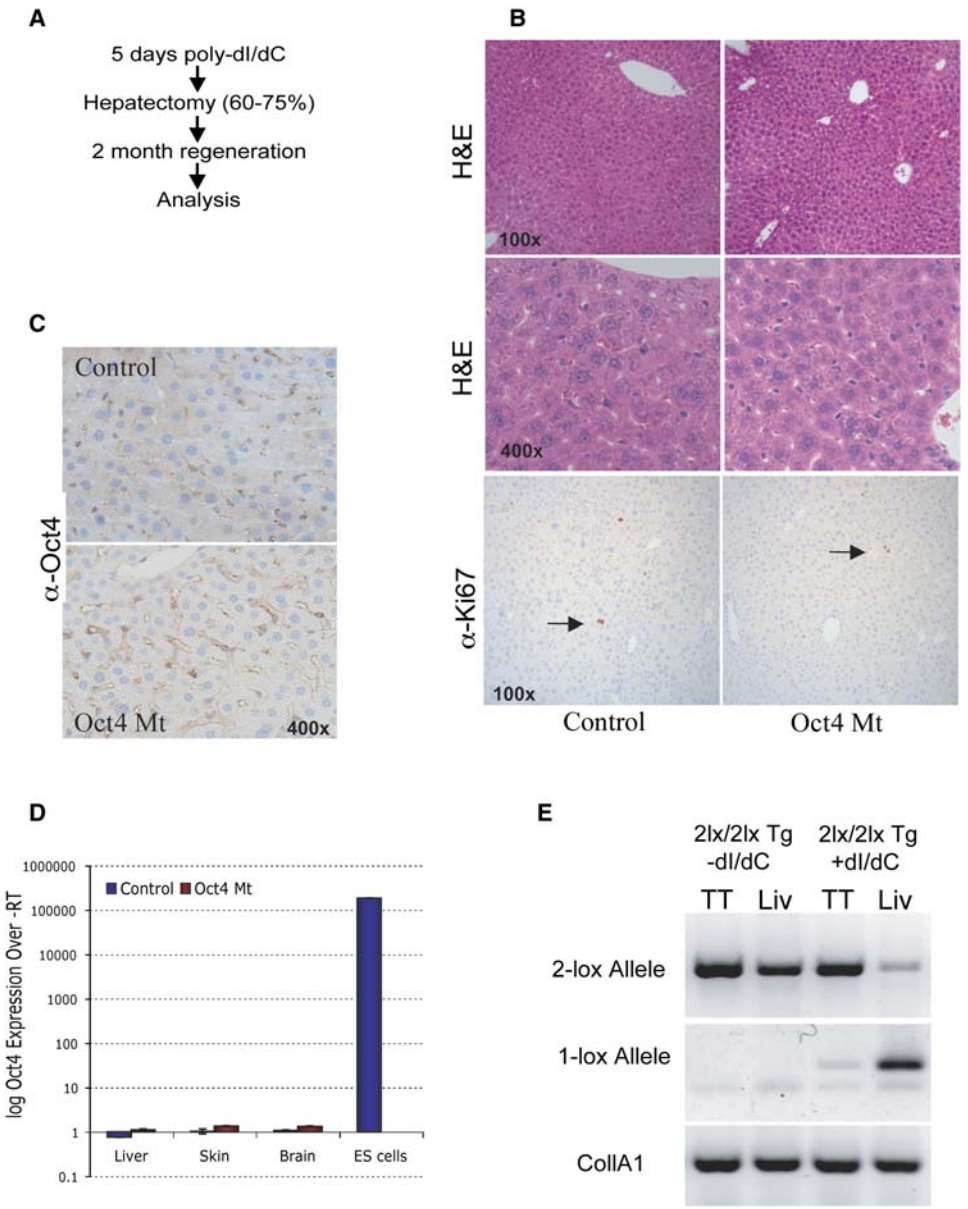

Figure 4. Liver Regeneration after *Mx1-Cre*-Mediated Inactivation of *Oct4*

(A) Outline of experimental design for liver regeneration in *Oct4* mutant and control *Mx1-Cre* mice.

(B) Histological analysis of regenerated liver in the presence or absence of *Oct4*. Hematoxylin and eosin (H&E) staining at low (top panels) and high (middle panels) magnification demonstrating normal liver architecture with well-formed hepatic lobules, bile ducts, and vessels after regeneration. Ki67 staining (lower panels, arrows) showing a normal distribution of proliferating cells in regenerated liver 2 months after hepatectomy.

(C) Oct4 immunostaining of newly generated liver revealed no Oct4+ nuclei, however some non-specific staining of extracellular matrix was observed in both control and mutant liver.

(D) qRT-PCR analysis of control and *Oct4* mutant liver, skin, and brain reveals no significant *Oct4* expression in comparison to ES cells. Data are mean ± SD, relative to –RT, n = 3.

(E) PCR analysis of the *Oct4* locus in genomic DNA isolated from tail tip (TT) or hepatic tissue 2 months after hepatectomy (Liv) showing the presence of the mutant *1-lox* allele and absence of the functional *2-lox* allele. The *type I collagen* gene acts as a loading control.

reactivation of endogenous *Oct4* regulatory elements (Yamaguchi et al., 2005). These observations are consistent with the notion that the epigenetic mechanisms silencing *Oct4* in somatic tissues are highly effective and that *Oct4* is dispensable in the adult, and is only rarely activated in somatic tumors.

What then could be the significance of somatic *Oct4* expression observed in numerous studies? We note that the *Oct4* expression levels described in many of these studies were very low, usually detected only after 30–40 cycles of PCR amplification (Table S1). We confirmed published results in that we were able to detect low levels

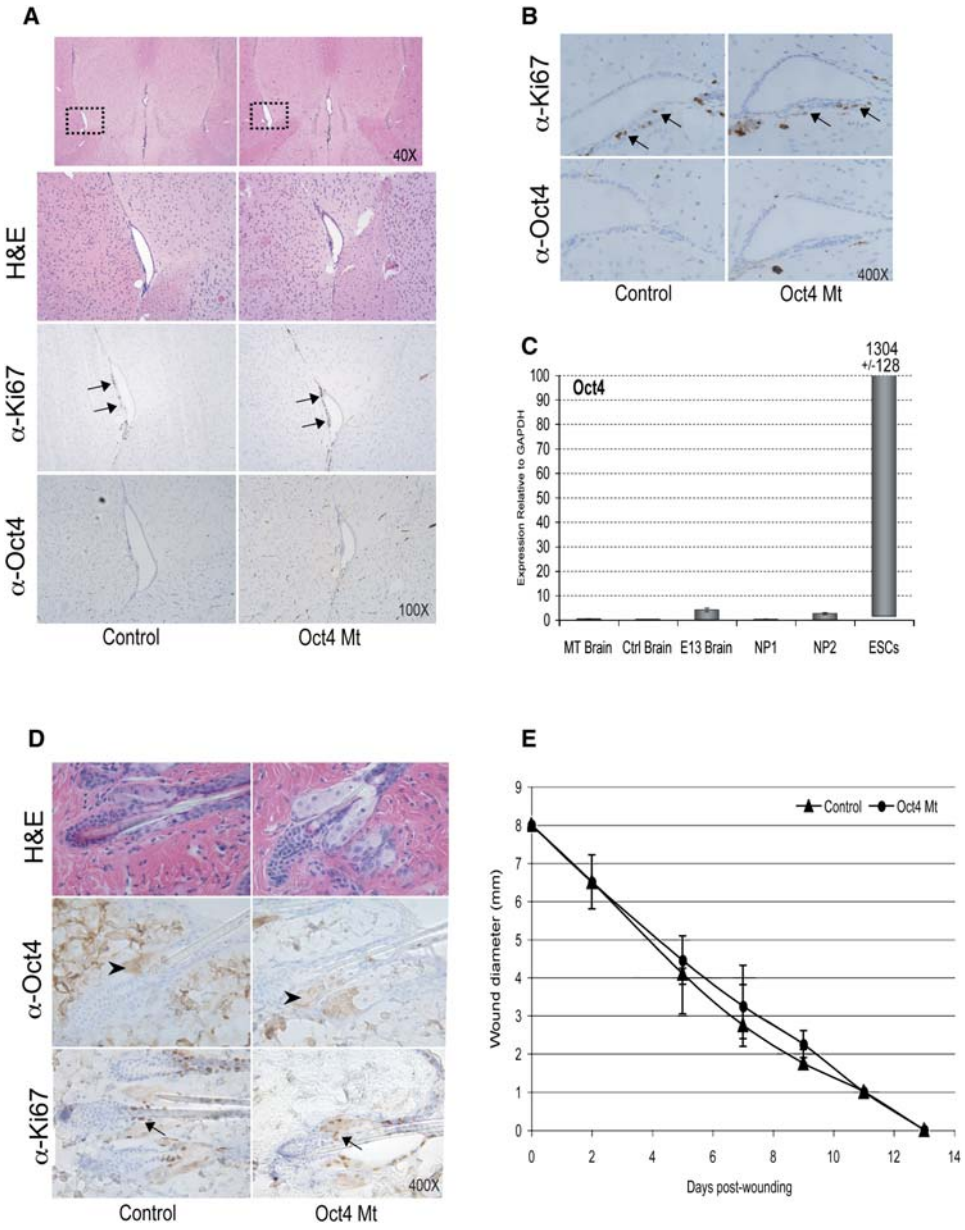

Figure 5. CNS Analysis in *Oct4* Conditional, *Nestin-Cre* Mice and Hair Follicle Analysis in *Oct4* Conditional, *K15-CrePr1* Mice

(A) Coronal sections of control or *Oct4* mutant brain isolated from 14-month-old mice reveal no gross morphological abnormalities. The subventricular zone of the lateral ventricles reveals proliferating neural progenitor cells by Ki67 staining (arrows). Oct4 immunostaining revealed no positive nuclei; however, nonspecific staining of vascularization was observed in both control and mutant brains.

(B) High magnification image of lateral ventricles described in (A).

(C) Quantitative RT-PCR analysis of *Oct4* expression in control and mutant brain, wild-type embryonic day 13.5 brain, and two lines of ex vivo cultured primary neural progenitor cell lines NP1 and NP2 revealed no significant *Oct4* mRNA in any of these samples in comparison to ESCs. Data are mean ± SD, relative to GAPDH, n = 3.

(D) Sections of control and *K15-CrePr1Pr1 Oct4* mutant hair follicles show no Oct4+ nuclei but rather diffuse, nonspecific Oct4 staining in sebocytes (center panels, arrowheads). Ki67 immunostaining of follicles shows proliferative cells in both control and mutant follicles (lower panels, arrows).

(E) Wound-healing assays in which 8 mm, full thickness dermal punches were monitored for 2 weeks, n = 3.

of *Oct4* message in various progenitor cells and somatic tissue (including HSCs, MSCs, intestinal crypt progenitors, and neuroprogenitors) by quantitative RT-PCR. The amount of *Oct4* detected was many fold lower than what was observed in ES cells and present even in samples that had genetically inactive *Oct4* loci, raising the question as to whether the observed *Oct4* expression is functionally significant or merely represents the noise of the detection method. Furthermore, the genome contains at least six *Oct4* pseudogenes, the expression of which could

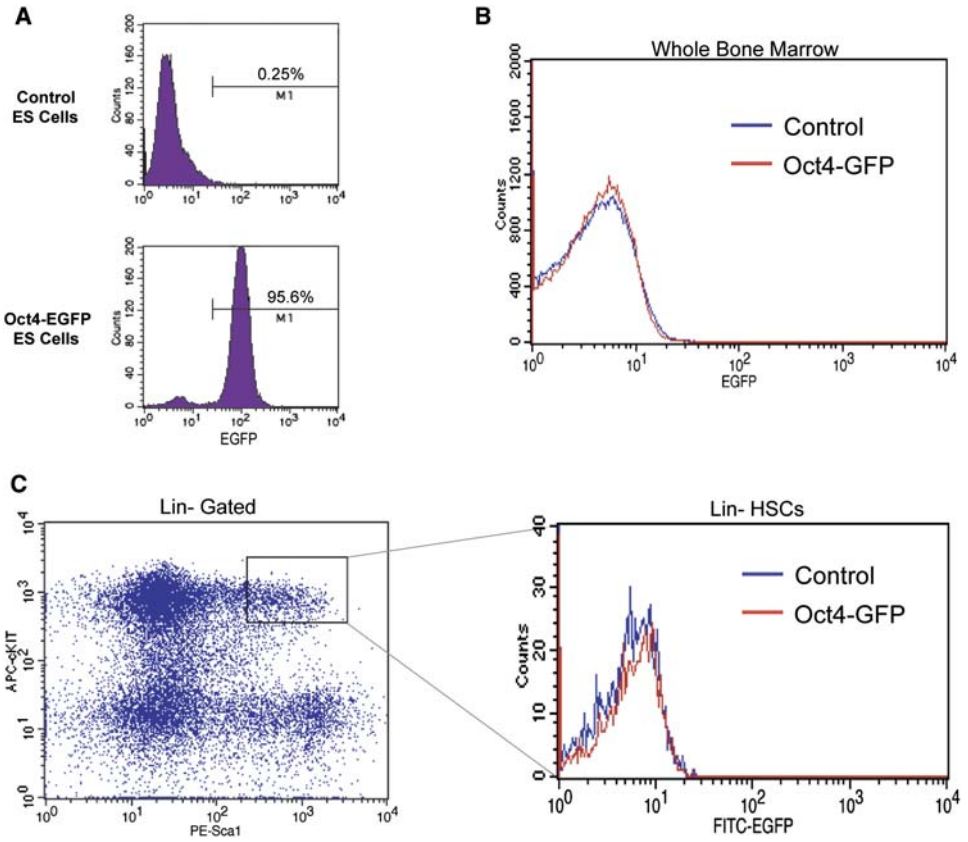

Figure 6. *Oct4* Gene Expression in Bone Marrow and HSCs

(A) Flow cytometric analysis for GFP activity in control and *Oct4-EGFP* targeted ES cells.

(B) *Oct4-EGFP* activity in total bone marrow isolated from *Oct4-EGFP* mice showing no discernible differences in the number of GFP-positive cells.

(C) *Oct4-EGFP* activity in c-Kit+, Sca+, Lin− HSCs is undetectable.

potentially be mistaken for that of the endogenous *Oct4* gene (Pain et al., 2005; Suo et al., 2005). In addition to *Oct4* pseudogenes, a number of Pou-domain family members are expressed in somatic tissue, and similarities in both gene and protein sequence may also contribute to false detection of *Oct4* in a number of assays. This caveat is evident in the immunohistochemistry presented in the current study. Using an *Oct4* antibody, we were able to detect positive cells in several tissues, particularly the stroma of the intestine. It is clear that this staining is nonspecific, as it appeared in tissues lacking a functional *Oct4* locus and was not reproducible when using expression analysis or a GFP antibody in tissue sections isolated from *Oct4-GFP* mice. This also raises the issue of functional redundancy within the *Oct* family, such that the observed lack of phenotype in *Oct4* mutant tissue could be due to compensation by other Oct proteins, although we believe this possibility to be unlikely due to the evolutionary divergence between *Oct4* and these family members. Finally, the detection of *Oct4* expression in tumor cell lines and in vitro cultures of tissue-derived cells may be of little relevance to somatic stem cell function or carcinogenesis in vivo. It is possible, for example, that *Oct4* gene activation in cultured cells is a rare event and that *Oct4*-expressing cells may have a proliferative advantage in culture. In summary, our data strongly argue that *Oct4*, even if expressed at low levels in somatic cells, is dispensable for the self-renewal of somatic stem cells, for tissue homeostasis, and for the regeneration of tissue in the adult.

EXPERIMENTAL PROCEDURES

Generation and Maintenance of Mice

Conditional *Oct4* mice were maintained and genotyped as described previously (Kehler et al., 2004). *Nestin-Cre* mice were maintained and genotyped as previously described (Bates et al., 1999). In order to achieve 100% recombination of the target allele in neural progenitor cells, the imprinted *Nestin-Cre* transgene was passed through the male germline. *Mx1-Cre* mice were obtained from Jackson Labs (Bar Harbor, ME, USA). Activation of *Mx1-Cre* was achieved through five consecutive daily intraperitoneal injections of 0.5 mg polyinosinic-polycytidylic acid (poly dI/dC, Sigma, St. Louis, MO, USA). Partial hepatectomies were performed after *Mx1-Cre* activation on 8-week-old mice anesthetized with Avertin at a concentration of 0.5 mg/g. Regenerated hepatic tissue was isolated after an 8 week period during which mice were kept in sterile cages with antibiotic-containing water. *Villin-CreER* mice were a generous gift from Dr. Sylvie Robine at the Institut Curie, Paris, France. The *Villin-CreER* transgene was activated through five consecutive daily intraperitoneal injections of tamoxifen

(1 mg in corn oil) (Sigma). *K15-CrePr1Pr1* mice were a generous gift from Dr. George Cotsarelis at the University of Pennsylvania, Philadelphia, PA, USA. The *K15-CrePr1Pr1* transgene was activated through administration of 1% w/w mifepristone (Sigma) in hand cream directly to the dermis for five consecutive days. Dermal biopsies were performed 1 to 2 weeks after *K15-CrePr1Pr1* activation and monitored for 2 weeks for wound-healing ability with a micrometer.

Oct4-GFP mice were generated by subcloning a 6.5 kb genomic fragment encompassing exons 2–5 from a BAC library into Bluescript via HindIII and EcoRI sites and termed pBS-*Oct4*. A loxP-flanked pgk-Neo resistance cassette was cloned into the NotI site of *pIRES-EGFP*, and subsequently the portion containing *IRES-EGFP-floxed NEO* (lacking the polyA) was released via BamHI and EcoRV and subcloned into the unique BclI site of pBS-*Oct4* which lies between the stop codon and the polyadenylation signal. The targeting construct was linearized with SacII and electroporated into V6.5 ES cells. GFP-positive colonies were picked and correct integration was verified by Southern blot analysis on genomic DNA digested with BamHI and probed with a fragment released from pBS-*Oct4* with HindIII and SacI (5′ probe), resulting in a 6 kb wild-type band and a 9 kb targeted band. Targeted ES cells were transiently electroporated with Pac-Cre to eliminate the floxed Neo cassette. Clones that had excised the neo cassette gave a 7.4 kb band after digestion of genomic DNA with BamHI using the 5′ probe. All animals were treated in accordance with IACUC guidelines under current approved protocols.

Histological Analysis

Isolated tissues were fixed in 4% paraformaldehyde in phosphate-buffered saline (brain) or 10% phosphate-buffered formalin (all other tissue) overnight and subsequently embedded in paraffin wax using a Tissue-Tek VIP embedding machine (Miles Scientific, Napervielle, IL) and a Thermo Shandon Histocenter 2 (Thermo Fisher Scientific, Waltham, MA). Sections were cut at a thickness of 2 μm using a Leica RM2065 (Leica, Wetzlar, Germany) and stained with hematoxylin and eosin or antibodies against *Oct4* or *Ki67* as previously described (Hochedlinger et al., 2005). Tissues isolated from mice harboring an inducible *Oct4* cDNA under control of the reverse tetracycline transactivator were used as a positive control for Oct4 immunohistochemistry (Hochedlinger et al., 2005).

For immunofluorescence, cells were fixed in a 6-well plate with 4% PFA for 10 min. After one wash with PBS, the cells were blocked and permeabilized in 5% FBS, 0.1% Triton-X for 15 min. Cells were subsequently incubated with a primary antibody against Oct4 at a 1:100 dilution for 1 hr at room temperature (rabbit polyclonal, H-134; Santa Cruz Biotech, Santa Cruz, CA). After three washes with PBS, the cells were incubated with an anti-rabbit secondary antibody labeled with Cy3 for 1 hr in the dark. After a 5 min incubation with DAPI, the cells were washed three times with PBS.

Tissue Isolation and Marrow Cell Culture

Total intestinal epithelium was dissociated using a solution of 3 mM EDTA and 0.05 mM DTT for 30 min at room temperature. The musculature was discarded, and purified crypts/villi were used for DNA and RNA isolation. Fractionation of the crypt-villus structure to enrich for stem cells was performed as described in Ferraris et al. (1992). Ablation of intestinal epithelium was achieved through γ irradation of mice in a Gammacell-40 Exactor Low-Dose Research Irradiator using a dosage of 14 Gy. After irradiation, mice were monitored daily and euthanized no more than 8 days after irradiation. Neural progenitor cells were isolated by mechanical dissociation of E12.5 brains and cultured on polyornithine-coated tissue culture plastic in N3 media containing FGF and EGF (R&D Systems, Minneapolis, MN, USA) as described in Gritti et al. (2001). Whole marrow was isolated from 8-week-old mice from the femur and tibia after removal of the condyles at the growth plate by flushing with a syringe and 30-gauge needle containing DMEM + 5% fetal calf serum (FCS) (HyClone, Thermo Fisher Scientific). Whole marrow was separated into mesenchymal and hematopoietic fractions through differential plating on tissue culture plates for 72 hr in α-MEM supplemented with 15% FCS (HyClone). Colony formation (CFU-F) assays were carried out by plating 4×10^6 nucleated cells from freshly isolated whole marrow onto 10 cm plates and allowed to expand for 5 days, at which time cultures were stained with 0.1% Coomassie blue to identify colonies. For osteogenic differentiation, MSCs were plated at a density of 10^6 cells/6-well plate and allowed to proliferate until confluent, at which time osteogenesis was initiated by the addition of ascorbic acid and β-glycerol phosphate to the culture media (Owen et al., 1990). Alkaline phosphatase staining and silver nitrate staining for mineral by the method of Von Kossa were performed as previously described (Lengner et al., 2006). Chondrogenic differentiation of MSCs was carried out in high-density micromass cultures in the presence of 100 ng/ml BMP2 (R&D Systems) and analyzed as previously described (Lengner et al., 2004).

Hematopoietic Lineage Analysis and Flow Cytometry

For competitive reconstitution assays, C57Bl/6-CD45.1 recipient mice were lethally irradiated (11 Gy) with γ irradiation in a split dose, with 2 hr between doses. The reconstituting cells were injected retro-orbitally within 24 hr of irradiation. CD45.2 whole bone marrow cells (2×10^5) from either control or *Oct4* mutant mice were transplanted along with the same dose of "competitor" cells from B6-CD45.1 animals. Peripheral blood analysis was performed as previously described (Camargo et al., 2006). At various time points after transplantation, 200 μL peripheral blood was collected from the retro-orbital plexus of anesthetized transplant recipients. Erythrocytes were lysed and nucleated cells were simultaneously stained with anti-CD45.1, CD45.2, B220, Ly6G, and Mac1 antibodies. In order to identify HSCs, BM was stained with antibodies against c-Kit, Sca-1, Flt3, and a lineage cocktail (composed of CD3, B220, Ter119, Mac1, and Gr-1 antibodies). All antibodies were obtained from Ebiosciences (San Diego, CA). Stained blood and bone marrow samples were then analyzed by flow cytometry using a two-laser instrument, FACSCalibur (Becton Dickinson, Mountain View, CA), or sorted for subsequent RNA purification at the MIT FACS facility using a FACS Aria (Becton Dickinson). Differential blood counts were obtained with a Hemavet 850 (Drew Scientific, Oxford, CT).

Quantitative RT-PCR

Total RNA was isolated using Trizol reagent (Invitrogen, Carlsbad, CA). Five micrograms of total RNA was treated with DNase I to remove potential contamination of genomic DNA using a DNA Free RNA kit (Zymo Research, Orange, CA). One microgram of DNase I-treated RNA was reverse transcribed using a First Strand Synthesis kit (Invitrogen) and ultimately resuspended in 100 ul of water. Quantitative PCR analysis was performed in triplicate using 1/50 of the reverse transcription reaction in an ABI Prism 7000 (Applied Biosystems, Foster City, CA) with Platinum SYBR green qPCR SuperMix-UDG with ROX (Invitrogen). Primers used for *Oct4* amplification were as follows: F, 5′-ACATCGCCAATCAGCTTGG-3′; R, 5′-AGAACCATACTCGAACCACATCC-3′. To ensure equal loading of cDNA into RT reactions, GAPDH mRNA was amplified using the following: F, 5′-TTCACCACCATGGAGAAGGC-3′; and R, 5′-CCCTTTTGGCTCCACCCT-3′. Data were extracted from the linear range of amplification. All graphs of qRT-PCR data shown represent samples of RNA that were DNase treated, reverse transcribed, and amplified in parallel to avoid variation inherent in these procedures.

Supplemental Data

Supplemental Data include one table and three figures and can be found with this article online at http://www.cellstemcell.com/cgi/content/full/1/4/403/DC1/.

ACKNOWLEDGMENTS

The authors would like to thank Jessica Dausman for assistance with animal husbandry and surgery, Dongdong Fu for histological processing, Jonathan Johnnidis for assistance with flow cytometric analyses,

and the Jaenisch lab for critical comments on the manuscript. This work is supported by NIH grants RO1-CA087869, R37-CA084198, and RO1-HD0445022, and by a grant from Philip Morris International. C.J.L. is supported by an NIH Ruth L. Kirschstein NRSA F32-CA119647.

Received: March 8, 2007
Revised: June 11, 2007
Accepted: July 27, 2007
Published: October 10, 2007

REFERENCES

Bates, B., Rios, M., Trumpp, A., Chen, C., Fan, G., Bishop, J.M., and Jaenisch, R. (1999). Neurotrophin-3 is required for proper cerebellar development. Nat. Neurosci. *2*, 115–117.

Belting, H.G., Hauptmann, G., Meyer, D., Abdelilah-Seyfried, S., Chitnis, A., Eschbach, C., Soll, I., Thisse, C., Thisse, B., Artinger, K.B., et al. (2001). spiel ohne grenzen/pou2 is required during establishment of the zebrafish midbrain-hindbrain boundary organizer. Development *128*, 4165–4176.

Beltrami, A.P., Cesselli, D., Bergamin, N., Marcon, P., Rigo, S., Puppato, E., D'Aurizio, F., Verardo, R., Piazza, S., Pignatelli, A., et al. (2007). Multipotent cells can be generated in vitro from several adult human organs (heart, liver and bone marrow). Blood, in press. Published online May 24, 2007. 10.1182/blood-2006-11-055566.

Boyer, L.A., Lee, T.I., Cole, M.F., Johnstone, S.E., Levine, S.S., Zucker, J.P., Guenther, M.G., Kumar, R.M., Murray, H.L., Jenner, R.G., et al. (2005). Core transcriptional regulatory circuitry in human embryonic stem cells. Cell *122*, 947–956.

Camargo, F.D., Chambers, S.M., Drew, E., McNagny, K.M., and Goodell, M.A. (2006). Hematopoietic stem cells do not engraft with absolute efficiencies. Blood *107*, 501–507.

Cervello, I., Martinez-Conejero, J.A., Horcajadas, J.A., Pellicer, A., and Simon, C. (2006). Identification, characterization and co-localization of label-retaining cell population in mouse endometrium with typical undifferentiated markers. Hum. Reprod. *22*, 45–51.

Davis, S.F., Hood, J., Thomas, A., and Bunnell, B.A. (2006). Isolation of adult rhesus neural stem and progenitor cells and differentiation into immature oligodendrocytes. Stem Cells Dev. *15*, 191–199.

D'Ippolito, G., Diabira, S., Howard, G.A., Menei, P., Roos, B.A., and Schiller, P.C. (2004). Marrow-isolated adult multilineage inducible (MIAMI) cells, a unique population of postnatal young and old human cells with extensive expansion and differentiation potential. J. Cell Sci. *117*, 2971–2981.

D'Ippolito, G., Diabira, S., Howard, G.A., Roos, B.A., and Schiller, P.C. (2006). Low oxygen tension inhibits osteogenic differentiation and enhances stemness of human MIAMI cells. Bone *39*, 513–522.

Dyce, P.W., Zhu, H., Craig, J., and Li, J. (2004). Stem cells with multilineage potential derived from porcine skin. Biochem. Biophys. Res. Commun. *316*, 651–658.

Dyce, P.W., Wen, L., and Li, J. (2006). In vitro germline potential of stem cells derived from fetal porcine skin. Nat. Cell Biol. *8*, 384–390.

el Marjou, F., Janssen, K.P., Chang, B.H., Li, M., Hindie, V., Chan, L., Louvard, D., Chambon, P., Metzger, D., and Robine, S. (2004). Tissue-specific and inducible Cre-mediated recombination in the gut epithelium. Genesis *39*, 186–193.

Fan, G., Beard, C., Chen, R.Z., Csankovszki, G., Sun, Y., Siniaia, M., Biniszkiewicz, D., Bates, B., Lee, P.P., Kuhn, R., et al. (2001). DNA hypomethylation perturbs the function and survival of CNS neurons in postnatal animals. J. Neurosci. *21*, 788–797.

Feldman, N., Gerson, A., Fang, J., Li, E., Zhang, Y., Shinkai, Y., Cedar, H., and Bergman, Y. (2006). G9a-mediated irreversible epigenetic inactivation of Oct-3/4 during early embryogenesis. Nat. Cell Biol. *8*, 188–194.

Ferraris, R.P., Villenas, S.A., and Diamond, J. (1992). Regulation of brush-border enzyme activities and enterocyte migration rates in mouse small intestine. Am. J. Physiol. *262*, G1047–G1059.

Gidekel, S., Pizov, G., Bergman, Y., and Pikarsky, E. (2003). Oct-3/4 is a dose-dependent oncogenic fate determinant. Cancer Cell *4*, 361–370.

Goolsby, J., Marty, M.C., Heletz, D., Chiappelli, J., Tashko, G., Yarnell, D., Fishman, P.S., Dhib-Jalbut, S., Bever, C.T., Jr., Pessac, B., and Trisler, D. (2003). Hematopoietic progenitors express neural genes. Proc. Natl. Acad. Sci. USA *100*, 14926–14931.

Gritti, A., Galli, R., and Vescovi, A.L. (2001). Cultures of stem cells from the central nervous system. In Protocols for Neural Cell Culture, S. Fedoroff and A. Richardson, eds. (Totowa, NJ: Humana Press), pp. 173–185.

Gupta, S., Verfaillie, C., Chmielewski, D., Kren, S., Eidman, K., Connaire, J., Heremans, Y., Lund, T., Blackstad, M., Jiang, Y., et al. (2006). Isolation and characterization of kidney-derived stem cells. J. Am. Soc. Nephrol. *17*, 3028–3040.

Hochedlinger, K., Yamada, Y., Beard, C., and Jaenisch, R. (2005). Ectopic expression of Oct-4 blocks progenitor-cell differentiation and causes dysplasia in epithelial tissues. Cell *121*, 465–477.

Ito, M., Liu, Y., Yang, Z., Nguyen, J., Liang, F., Morris, R.J., and Cotsarelis, G. (2005). Stem cells in the hair follicle bulge contribute to wound repair but not to homeostasis of the epidermis. Nat. Med. *11*, 1351–1354.

Izadpanah, R., Trygg, C., Patel, B., Kriedt, C., Dufour, J., Gimble, J.M., and Bunnell, B.A. (2006). Biologic properties of mesenchymal stem cells derived from bone marrow and adipose tissue. J. Cell Biochem. *99*, 1285–1297.

Jiang, Y., Jahagirdar, B.N., Reinhardt, R.L., Schwartz, R.E., Keene, C.D., Ortiz-Gonzalez, X.R., Reyes, M., Lenvik, T., Lund, T., Blackstad, M., et al. (2002). Pluripotency of mesenchymal stem cells derived from adult marrow. Nature *418*, 41–49.

Johnson, J., Bagley, J., Skaznik-Wikiel, M., Lee, H.J., Adams, G.B., Niikura, Y., Tschudy, K.S., Tilly, J.C., Cortes, M.L., Forkert, R., et al. (2005). Oocyte generation in adult mammalian ovaries by putative germ cells in bone marrow and peripheral blood. Cell *122*, 303–315.

Keating, A. (2006). Mesenchymal stromal cells. Curr. Opin. Hematol. *13*, 419–425.

Kehler, J., Tolkunova, E., Koschorz, B., Pesce, M., Gentile, L., Boiani, M., Lomeli, H., Nagy, A., McLaughlin, K.J., Scholer, H.R., and Tomilin, A. (2004). Oct4 is required for primordial germ cell survival. EMBO Rep. *5*, 1078–1083.

Kondo, M., Wagers, A.J., Manz, M.G., Prohaska, S.S., Scherer, D.C., Beilhack, G.F., Shizuru, J.A., and Weissman, I.L. (2003). Biology of hematopoietic stem cells and progenitors: implications for clinical application. Annu. Rev. Immunol. *21*, 759–806.

Kues, W.A., Petersen, B., Mysegades, W., Carnwath, J.W., and Niemann, H. (2005). Isolation of murine and porcine fetal stem cells from somatic tissue. Biol. Reprod. *72*, 1020–1028.

Kuhn, R., Schwenk, F., Aguet, M., and Rajewsky, K. (1995). Inducible gene targeting in mice. Science *269*, 1427–1429.

Lamoury, F.M., Croitoru-Lamoury, J., and Brew, B.J. (2006). Undifferentiated mouse mesenchymal stem cells spontaneously express neural and stem cell markers Oct-4 and Rex-1. Cytotherapy *8*, 228–242.

Lengner, C.J., Lepper, C., van Wijnen, A.J., Stein, J.L., Stein, G.S., and Lian, J.B. (2004). Primary mouse embryonic fibroblasts: a model of mesenchymal cartilage formation. J. Cell. Physiol. *200*, 327–333.

Lengner, C.J., Steinman, H.A., Gagnon, J., Smith, T.W., Henderson, J.E., Kream, B.E., Stein, G.S., Lian, J.B., and Jones, S.N. (2006). Osteoblast differentiation and skeletal development are regulated by Mdm2-p53 signaling. J. Cell Biol. *172*, 909–921.

Ling, T.Y., Kuo, M.D., Li, C.L., Yu, A.L., Huang, Y.H., Wu, T.J., Lin, Y.C., Chen, S.H., and Yu, J. (2006). Identification of pulmonary Oct-4+ stem/progenitor cells and demonstration of their susceptibility to SARS coronavirus (SARS-CoV) infection in vitro. Proc. Natl. Acad. Sci. USA *103*, 9530–9535.

Loh, Y.H., Wu, Q., Chew, J.L., Vega, V.B., Zhang, W., Chen, X., Bourque, G., George, J., Leong, B., Liu, J., et al. (2006). The Oct4 and Nanog transcription network regulates pluripotency in mouse embryonic stem cells. Nat. Genet. *38*, 431–440.

Looijenga, L.H., Stoop, H., de Leeuw, H.P., de Gouveia Brazao, C.A., Gillis, A.J., van Roozendaal, K.E., van Zoelen, E.J., Weber, R.F., Wolffenbuttel, K.P., van Dekken, H., et al. (2003). POU5F1 (OCT3/4) identifies cells with pluripotent potential in human germ cell tumors. Cancer Res. *63*, 2244–2250.

Matthai, C., Horvat, R., Noe, M., Nagele, F., Radjabi, A., van Trotsenburg, M., Huber, J., and Kolbus, A. (2006). Oct-4 expression in human endometrium. Mol. Hum. Reprod. *12*, 7–10.

Mongan, N.P., Martin, K.M., and Gudas, L.J. (2006). The putative human stem cell marker, Rex-1 (Zfp42): structural classification and expression in normal human epithelial and carcinoma cell cultures. Mol. Carcinog. *45*, 887–900.

Moriscot, C., de Fraipont, F., Richard, M.J., Marchand, M., Savatier, P., Bosco, D., Favrot, M., and Benhamou, P.Y. (2005). Human bone marrow mesenchymal stem cells can express insulin and key transcription factors of the endocrine pancreas developmental pathway upon genetic and/or microenvironmental manipulation in vitro. Stem Cells *23*, 594–603.

Morris, R.J., Liu, Y., Marles, L., Yang, Z., Trempus, C., Li, S., Lin, J.S., Sawicki, J.A., and Cotsarelis, G. (2004). Capturing and profiling adult hair follicle stem cells. Nat. Biotechnol. *22*, 411–417.

Nayernia, K., Lee, J.H., Drusenheimer, N., Nolte, J., Wulf, G., Dressel, R., Gromoll, J., and Engel, W. (2006). Derivation of male germ cells from bone marrow stem cells. Lab. Invest. *86*, 654–663.

Nichols, J., Zevnik, B., Anastassiadis, K., Niwa, H., Klewe-Nebenius, D., Chambers, I., Scholer, H., and Smith, A. (1998). Formation of pluripotent stem cells in the mammalian embryo depends on the POU transcription factor Oct4. Cell *95*, 379–391.

Okuda, T., Tagawa, K., Qi, M.L., Hoshio, M., Ueda, H., Kawano, H., Kanazawa, I., Muramatsu, M., and Okazawa, H. (2004). Oct-3/4 repression accelerates differentiation of neural progenitor cells in vitro and in vivo. Brain Res. Mol. Brain Res. *132*, 18–30.

Owen, T.A., Aronow, M., Shalhoub, V., Barone, L.M., Wilming, L., Tassinari, M.S., Kennedy, M.B., Pockwinse, S., Lian, J.B., and Stein, G.S. (1990). Progressive development of the rat osteoblast phenotype in vitro: reciprocal relationships in expression of genes associated with osteoblast proliferation and differentiation during formation of the bone extracellular matrix. J. Cell. Physiol. *143*, 420–430.

Pain, D., Chirn, G.W., Strassel, C., and Kemp, D.M. (2005). Multiple retropseudogenes from pluripotent cell-specific gene expression indicates a potential signature for novel gene identification. J. Biol. Chem. *280*, 6265–6268.

Pallante, B.A., Duignan, I., Okin, D., Chin, A., Bressan, M.C., Mikawa, T., and Edelberg, J.M. (2007). Bone marrow Oct3/4+ cells differentiate into cardiac myocytes via age-dependent paracrine mechanisms. Circ. Res. *100*, e1–e11.

Pochampally, R.R., Smith, J.R., Ylostalo, J., and Prockop, D.J. (2004). Serum deprivation of human marrow stromal cells (hMSCs) selects for a subpopulation of early progenitor cells with enhanced expression of OCT-4 and other embryonic genes. Blood *103*, 1647–1652.

Redvers, R.P., Li, A., and Kaur, P. (2006). Side population in adult murine epidermis exhibits phenotypic and functional characteristics of keratinocyte stem cells. Proc. Natl. Acad. Sci. USA *103*, 13168–13173.

Ren, H., Cao, Y., Zhao, Q., Li, J., Zhou, C., Liao, L., Jia, M., Cai, H., Han, Z.C., Yang, R., et al. (2006). Proliferation and differentiation of bone marrow stromal cells under hypoxic conditions. Biochem. Biophys. Res. Commun. *347*, 12–21.

Romagnani, P., Annunziato, F., Liotta, F., Lazzeri, E., Mazzinghi, B., Frosali, F., Cosmi, L., Maggi, L., Lasagni, L., Scheffold, A., et al. (2005). CD14+CD34low cells with stem cell phenotypic and functional features are the major source of circulating endothelial progenitors. Circ. Res. *97*, 314–322.

Sagrinati, C., Netti, G.S., Mazzinghi, B., Lazzeri, E., Liotta, F., Frosali, F., Ronconi, E., Meini, C., Gacci, M., Squecco, R., et al. (2006). Isolation and characterization of multipotent progenitor cells from the Bowman's capsule of adult human kidneys. J. Am. Soc. Nephrol. *17*, 2443–2456.

Schneider, A., Zhang, Y., Guan, Y., Davis, L.S., and Breyer, M.D. (2003). Differential, inducible gene targeting in renal epithelia, vascular endothelium, and viscera of Mx1Cre mice. Am. J. Physiol. Renal Physiol. *284*, F411–F417.

Serafini, M., Dylla, S.J., Oki, M., Heremans, Y., Tolar, J., Jiang, Y., Buckley, S.M., Pelacho, B., Burns, T.C., Frommer, S., et al. (2007). Hematopoietic reconstitution by multipotent adult progenitor cells: precursors to long-term hematopoietic stem cells. J. Exp. Med. *204*, 129–139.

Suo, G., Han, J., Wang, X., Zhang, J., Zhao, Y., and Dai, J. (2005). Oct4 pseudogenes are transcribed in cancers. Biochem. Biophys. Res. Commun. *337*, 1047–1051.

Tai, M.H., Chang, C.C., Kiupel, M., Webster, J.D., Olson, L.K., and Trosko, J.E. (2005). Oct4 expression in adult human stem cells: evidence in support of the stem cell theory of carcinogenesis. Carcinogenesis *26*, 495–502.

Thomas, T., Nowka, K., Lan, L., and Derwahl, M. (2006). Expression of endoderm stem cell markers: evidence for the presence of adult stem cells in human thyroid glands. Thyroid *16*, 537–544.

Tondreau, T., Meuleman, N., Delforge, A., Dejeneffe, M., Leroy, R., Massy, M., Mortier, C., Bron, D., and Lagneaux, L. (2005). Mesenchymal stem cells derived from CD133-positive cells in mobilized peripheral blood and cord blood: proliferation, Oct4 expression, and plasticity. Stem Cells *23*, 1105–1112.

Walkup, M.H., and Gerber, D.A. (2006). Hepatic stem cells: in search of. Stem Cells *24*, 1833–1840.

Wang, R., Li, J., and Yashpal, N. (2004). Phenotypic analysis of c-Kit expression in epithelial monolayers derived from postnatal rat pancreatic islets. J. Endocrinol. *182*, 113–122.

Wang, J., Rao, S., Chu, J., Shen, X., Levasseur, D.N., Theunissen, T.W., and Orkin, S.H. (2006). A protein interaction network for pluripotency of embryonic stem cells. Nature *444*, 364–368.

Yamaguchi, S., Yamazaki, Y., Ishikawa, Y., Kawaguchi, N., Mukai, H., and Nakamura, T. (2005). EWSR1 is fused to POU5F1 in a bone tumor with translocation t(6;22)(p21;q12). Genes Chromosomes Cancer *43*, 217–222.

Yu, H., Fang, D., Kumar, S.M., Li, L., Nguyen, T.K., Acs, G., Herlyn, M., and Xu, X. (2006). Isolation of a novel population of multipotent adult stem cells from human hair follicles. Am. J. Pathol. *168*, 1879–1888.

Zhang, S., Jia, Z., Ge, J., Gong, L., Ma, Y., Li, T., Guo, J., Chen, P., Hu, Q., Zhang, P., et al. (2005). Purified human bone marrow multipotent mesenchymal stem cells regenerate infarcted myocardium in experimental rats. Cell Transplant. *14*, 787–798.